Magnetic Relaxations in Metallic Multilayers

Bret Heinrich, Radovan Urban, and Georg Woltersdorf

***Abstract*—The intrinsic damping mechanism in metals caused by incoherent scattering of itinerant electron-hole pair excitations by phonons and magnons will be reviewed. The unique features of magnetic relaxations in multilayers were studied by ferromagnetic resonance (FMR) using magnetic single, Au–Fe–GaAs(001), and double layer Au–Fe–Au–Fe–GaAs(001) structures prepared by molecular beam epitaxy. The magnetic relaxation in single-layer films is described by the Gilbert damping with no extrinsic contributions to the FMR linewidth. These films provided an excellent opportunity to investigate nonlocal damping. The main result of these studies is that ultrathin Fe films in magnetic double layers acquire an additional interface Gilbert damping. This is in agreement with recent predictions of nonlocal interface damping which is based on the transport of spin angular momentum between the ferromagnetic layers. Measurements of the nonlocal Gilbert damping offer a possibility to carry out quantitative studies of the relaxation torques caused by nonlocal spin momentum transfer. Numerical simulations of magnetization reversal and stationary precession for an applied perpendicular current in Au–Fe–Au–Fe–GaAs(001) multilayers will be shown.**

***Index Terms*—Ferromagnetic resonance, magnetic multilayers, nonlocal spin relaxations.**

I. Introduction

THE SMALL lateral dimensions of spintronic devices and high density memory bits require the use of magnetic metallic ultrathin film structures where the magnetic moments across the film are locked together by exchange coupling. Spintronics and high density magnetic recording employ fast magnetization reversal processes. It is currently of considerable interest to acquire a thorough understanding of the spin dynamics and magnetic relaxation processes in the nanosecond time regime. The purpose of this paper is to review the basic concepts of magnetic relaxations in metallic ferromagnets.

The spin dynamics in the classical limit can be described by the Landau–Lifshitz (LL) equation of motion

$$\frac{1}{\gamma}\frac{\partial \mathbf{M}}{\partial t} = -\left[\mathbf{M}\times\mathbf{H}_{\text{eff}}\right] - \frac{\lambda}{\gamma M_s^2}\left[\mathbf{M}\times\mathbf{M}\times\mathbf{H}_{\text{eff}}\right] \quad (1)$$

where γ is the absolute value of the electron spectroscopic splitting factor, M_s is the saturation magnetization and λ is the LL damping parameter. The effective field $\mathbf{H}_{\text{eff}}$ is given by [1]–[4]

$$\mathbf{H}_{\text{eff}} = -\frac{\partial U}{\partial \mathbf{M}} \quad (2)$$

Manuscript received February 14, 2002. This work was supported by the Natural Science and Engineering Research Council of Canada (NSERC) and by the Canadian Institute for Advanced Research (CIAR).

The authors are with the Physics Department, Simon Fraser University, Burnaby, BC V5A 1S6, Canada (e-mail: bheinric@sfu.ca).

Digital Object Identifier 10.1109/TMAG.2002.801906.

where U is the Gibbs energy of the system which includes the Zeeman energy of the external dc field $\mathbf{H}$ and external rf magnetic field h, all magnetic anisotropies and the inter-layer and intralayer exchange interaction energies. The first term on the right-hand side of (1) represents the precessional torque and the second term represents the well-known LL damping torque. For small damping $\alpha = \lambda/\gamma M_s \ll 1$, the LL damping term can be replaced by the Gilbert damping term, resulting in the Gilbert equation of motion

$$\frac{1}{\gamma}\frac{\partial \mathbf{M}}{\partial t} = -\left[\mathbf{M}\times\mathbf{H}_{\text{eff}}\right] + \frac{G}{\gamma^2 M_s^2}\left[\mathbf{M}\times\frac{\partial \mathbf{M}}{\partial t}\right] \quad (3)$$

where G is the Gilbert damping parameter. The relaxation parameter α is dimensionless and often used to represent the strength of magnetic damping. For an arbitrary strength of G the Gilbert damping can be converted into LL damping by the following [5]:

$$\lambda = G\frac{1}{1+\alpha_G^2} \quad \gamma_{LL} = \gamma_G\frac{1}{1+\alpha_G^2} \quad (4)$$

where $\alpha_G = G/(\gamma M_s)$. The Gilbert and LL damping equations of motion are identical for small damping, $\alpha_G \ll 1$.

A. Ferromagnetic Resonance (FMR) Linewidth

In the parallel FMR configuration, the static magnetization and the applied field are in the film plane. The FMR linewidth (using the half-width at half-maximum (HWHM) of absorbed microwave power) for the LL and Gilbert damping is given by

$$\Delta H = \left(\frac{G}{\gamma M_s}\right)\left(\frac{\omega}{\gamma}\right) = \cdot\alpha\cdot\frac{\omega}{\gamma}. \quad (5)$$

Note that the FMR linewidth is strictly linearly dependent on the microwave frequency ω and inversely proportional to the saturation magnetization M_s. The FMR linewidth increases proportionally with the damping coefficient α. With an increasing α, the Gilbert torque eventually becomes dominant and $\partial\mathbf{M}/\partial t \to 0$. For $\alpha \to \infty$ the system behaves like "molasses," approaching its equilibrium infinitely slowly. With an increasing λ the LL relaxation torque becomes dominant and $\mathbf{M}\times\mathbf{H}_{\text{eff}} \to 0$, i.e., the system is always in its quasiequilibrium state. This behavior does not seem to be realistic. Obviously, the Gilbert equation of motion is a more realistic description of damping in media with big losses $\alpha > 1$.

In the perpendicular FMR configuration, the static magnetization and the applied field are perpendicular to the film plane. The FMR linewidth is identical to that for the parallel configuration, see (5). This is a hallmark of the Gilbert and LL damping. The FMR linewidth is independent of the magnetization angle and it is proportional to the microwave frequency ω and inversely proportional to the saturation magnetization M_s.

II. Intrinsic Damping in Metals

A. Eddy Currents

In metallic films, the magnetic damping can be affected by eddy currents. The role of eddy currents in thin films can be estimated by evaluating the effective Gilbert damping accompanying the magnetization precession in the presence of eddy currents. For thin films where the rf magnetization response fully penetrates the film the contribution of eddy currents to G can be evaluated by integrating Maxwell's equations across the film thickness d. The resulting effective field has a Gilbert like form with the effective Gilbert damping, $G_{\rm eddy}$ (in Gauss's units)

$$\frac{G_{\rm eddy}}{(M_s\gamma)^2} = \frac{1}{6}\left(\frac{4\pi}{c}\right)^2 \sigma d^2 \tag{6}$$

where σ is the electrical conductivity and c is the velocity of light in free space. For Fe, the measured intrinsic Gilbert damping parameter is $G_{\rm Fe} \sim 0.5\times 10^8$ s^{-1} [6], [7]. The effective eddy current Gilbert parameter $G_{\rm eddy}$ becomes comparable to the intrinsic damping in Fe for a film thickness of 40 nm. Notice that $G_{\rm eddy}$ decreases rapidly with decreasing film thickness, $G_{\rm eddy}\sim d^2$. The ultrathin film limit in Fe is reasonably satisfied for $d < 10$ nm [8] and therefore the role of eddy currents is negligible in this case. For thicker films one has to solve the LL and Maxwell's equations selfconsistantly. The role of eddy currents in FMR for thicker films was quantitatively studied in [8]–[10].

B. Phonon Drag

The magnetization relaxation by a direct magnonphonon scattering is another possible damping mechanism. Suhl recently presented calculations for the magnon relaxation by phonon drag. His explicit results are limited to small geometries where the magnetization and lattice strain are homogeneous. Using the LL and lattice strain equations of motion in an asymptotic expansion, the Gilbert phonon damping G_{ph} is given by [11]

$$\frac{G_{ph}}{\gamma^2} = 2\eta\left(\frac{B_2(1+\nu)}{E}\right)^2 \tag{7}$$

where η is the phonon viscosity, B_2 is the magnetoelastic shear constant, E is Young's modulus and ν is the Poisson ratio. All parameters can be readily obtained except the parameter for the phonon viscosity η. However, it turns out that the phonon viscosity parameter η in the microwave range of frequencies was experimentally determined in our microwave transmission experiments, see [12]. In these studies at 9.5 GHz, a fast transversal elastic shear wave was generated by magnetoelastic coupling inside the skin depth of a 22-μm-thick Ni(001) crystal slab. The transversal elastic shear wave propagated across the slab and was then reradiated as transmitted microwave power at the other side of the Ni slab. We called this effect "phonon assisted microwave transmission." The experimental data were fitted using the LL and elastic wave equations of motion including the magnetoelastic coupling. The elastic wave relaxation time was found to be $\tau_{ph} = 6.6\times 10^{-10}$ s^{-1} at 9.5 GHz. The phonon viscosity as introduced in [11] is given by $\eta = c_{44}/\tau_{ph}\omega^2$, where c_{44} is the elastic modulus. For Ni $\eta = 3.4$ (in CGS). Using (7) results in a phonon Gilbert damping $G_{ph}\sim 10^7$ s^{-1}, that is ~ 30 times smaller than the intrinsic Gilbert damping parameter of Ni, $G_{Ni} = 2.4\times 10^8$ s^{-1}.

It should be pointed out that Suhl's theory does not treat the magnon-phonon interaction selfconsistenly. Selfconsistent calculations were carried out by Kobayashi *et al.* [13]. They showed that the magnetoelasticity can have only an appreciable effect on the FMR linewidth if the excited elastic wave establishes a resonant mode across the film thickness at or near the FMR field. This effect was called ferromagnetic elastic resonance (FMER). In Ni, the FMER effect can even result in a split FMR peak, see details in [13]. After an extensive and systematic effort to observe FMER in films of perfect Ni and Ni–Co platelets no convincing results were achieved. That indicates that the phonon resonance is hard to establish in real samples. The elastic wave wavelengths are $\sim$ 300 nm at 10 GHz. This means that for the magnetic films thinner than 150 nm at and below 10 GHz the FMER effect is absent.

The conclusion of the above two sections is that the contribution to the damping due to phonon drag and eddy currents are insufficient to explain the measured damping in magnetic metals. The eddy current losses are only important for thicker films and they can be neglected for ultrathin film samples, $d < 10$ nm, [14].

C. Spin Orbit Relaxation in Metallic Ferromagnets

The literature on intrinsic damping in metals dates back to the late sixties and seventies. The purpose of this section is not to get involved in details of calculations but rather to outline the underlying physics.

Kamberský [15] showed that the intrinsic damping in metallic ferromagnets can be treated by using the spin-orbit interaction Hamiltonian. The spin-orbit Hamiltonian corresponding to the transversal spin and angular momentum components can be expressed in a three-particle interaction Hamiltonian

$$\frac{1}{2}\sqrt{\frac{2S}{N}}\xi\sum_{\mathbf{k}}\sum_{\alpha,\alpha',\sigma}\left\langle\beta\left|L^+\right|\alpha\right\rangle c^+_{\beta,\mathbf{k}+\mathbf{q},\sigma}c_{\alpha,\mathbf{k},\sigma}b_{\mathbf{q}} + h.c. \tag{8}$$

where ξ is the coefficient of spin-orbit interaction, $L^+ = L_x + iL_y$ is the right handed component of the transversal atomic site angular momentum $\mathbf{L}_{a,t}$. $c_{\alpha,\mathbf{k},\sigma}$ and $c^+_{\beta,\mathbf{k}+\mathbf{q},\sigma}$ annihilate and create electrons in the appropriate Bloch states with the spin σ and $b_{\mathbf{q}}$ annihilates the spin wave with the wave-vector $\mathbf{q}$. The indexes α,β represent the projected local orbitals of Bloch states and are used to identify the individual electron bands. For simplicity, no dependence of the matrix elements $\langle\beta|L^+|\alpha\rangle$ on the wave-vectors will be considered. The RF susceptibility can be calculated by using Kubo–Green's function formalism in random phase approximation (RPA) [16]. The imaginary part of the denominator of the circularly polarized RF susceptibility for a spin wave with the wave-vector $\mathbf{q}$ and energy $\hbar\omega$ can be expressed in an effective damping field

$$\begin{aligned}\frac{G}{\gamma M_s}\frac{\omega}{\gamma} =& \frac{\langle S\rangle^2}{2M_s}\xi^2\left(\frac{1}{2\pi}\right)^3 \\ &\cdot\int d\mathbf{k}^3\sum_{\alpha,\beta,\sigma}\left\langle\beta\left|L^+\right|\alpha\right\rangle\left\langle\alpha\left|L^-\right|\beta\right\rangle \\ &\times\left(n_{\alpha,\mathbf{k},\sigma}-n_{\beta,\mathbf{k}+\mathbf{q},\sigma}\right)\delta\left(\hbar\omega+\varepsilon_{\alpha,\mathbf{k},\sigma}-\varepsilon_{\beta,\mathbf{k}+\mathbf{q},\sigma}\right).\end{aligned} \tag{9}$$

$\langle S\rangle$ is the reduced spin $S(M_s(T)/M_s(0))$. The difference in occupation numbers $\Delta n = n_{\alpha,\mathbf{k},\sigma} - n_{\beta,\mathbf{k+q},\sigma}$ is replaced by $\Delta n = (\partial n/\partial\varepsilon)\hbar\omega = \delta(\varepsilon_{\alpha,\mathbf{k},\sigma} - \varepsilon_F)\hbar\omega$ which confines the scattering processes in magnetic damping to the Fermi surface. The incoherent scattering of electron–hole pair excitations, $c^{+}_{\beta,\mathbf{k+q},\sigma}c_{\alpha,\mathbf{k},\sigma}$, can be treated by including an imaginary part in the electron–hole pair energy, $\varepsilon_{\alpha,\mathbf{k},\sigma} - \varepsilon_{\beta,\mathbf{k+q},\sigma} - i\hbar/\tau$. This broadens the delta function $\delta(\hbar\omega + \varepsilon_{\alpha,\mathbf{k},\sigma} - \varepsilon_{\beta,\mathbf{k+q},\sigma})$ into a Lorenzian [6]

$$\frac{\left(\frac{\hbar}{\tau}\right)}{\left(\hbar\omega + \varepsilon_{\alpha,\mathbf{k},\sigma} - \varepsilon_{\beta,\mathbf{k+q},\sigma}\right)^2 + \left(\frac{\hbar}{\tau}\right)^2}. \qquad (10)$$

The relaxation time τ can be viewed as a life time of electron–hole pair excitations. The Lorenzian function (10) should be looked upon as the probability of achieving a certain scattering event which is shown in the left bracket of this denominator. Since no spin flip is present during the scattering, the relaxation time τ corresponds to a simple lattice relaxation time which enters the conductivity. Note, that the effective damping field (9) is proportional to the frequency ω and inversely proportional to the saturation magnetization M_s as expected for Gilbert damping.

Intraband Transitions, $\alpha = \beta$: For low-frequency spin waves ($q \ll k_F$) the electron energy balance $\hbar\omega + \varepsilon_{\alpha,\mathbf{k},\sigma} - \varepsilon_{\alpha,\mathbf{k+q},\sigma} = \hbar\omega - \hbar^2/2m(2\mathbf{kq} + q^2)$ in the denominator of (10) can be significantly less than $\hbar/\tau$. This limit is satisfied, even in good crystalline structures, above cryogenic temperatures. After integration over the Fermi surface the Gilbert damping can be approximated by

$$G \simeq \langle S\rangle^2 \left(\frac{\xi}{\hbar}\right)^2 \left(\sum_\alpha \chi_P^\alpha \left\langle \alpha \left| L^+ \right| \alpha\right\rangle \left\langle \alpha \left| L^- \right| \alpha\right\rangle\right)\tau \qquad (11)$$

where χ_p^α are the Pauli susceptibilities of those states which participate in intraband electron transitions and satisfy $|\hbar\omega - \hbar^2/2m(2\mathbf{kq} + q^2)| \ll \hbar/\tau$. In this limit, the Gilbert damping is proportional to the relaxation time τ and consequently scales with conductivity.

Interband Transitions, $\alpha \neq \beta$: The interband transitions are accompanied with energy gaps $\Delta\varepsilon_{\beta,\alpha}$. The electron hole pair energy can be dominated by these gaps. For the gaps which are larger than the relaxation frequency $\hbar/\tau$ the Gilbert damping can be approximated by

$$G \simeq \langle S\rangle^2 \sum_\alpha \chi_P^\alpha \left(\Delta g_\alpha\right)^2 \frac{1}{\tau} \qquad (12)$$

where Δg_α is the deviation of the g-factor from its purely electronic value $g = 2$. $\Delta g_\alpha = 4\xi \sum_\beta \langle\alpha|L_x|\beta\rangle\langle\beta|L_x|\alpha\rangle/\Delta\varepsilon_{\beta,\alpha}$, see [17], determines the contribution of spin orbit interaction to the spectroscopic splitting factor γ. In this approximation, the Gilbert damping is proportional to $1/\tau$ and consequently scales with resistivity. In reality, a large distribution of energy gaps modifies the overall temperature dependence. The interband damping can be expected to be dependent on resistivity only at low temperatures. At higher temperatures the relaxation rate $\hbar/\tau$ becomes comparable to the energy gaps $\Delta\varepsilon_{\alpha,\beta}$, which results in a gradual saturation of the interband Gilbert damping with increasing temperature.

So far the treatment of intrinsic damping was mostly formal. At this point, it is useful to outline a simple physical description of intrinsic damping. Kamberský's model was originally based on the observation that the Fermi surface changes with the direction of the magnetization [18]. This model corresponds to the intraband transitions. This is relatively easy mechanism to describe by classical picture. As the precession of the magnetization evolves in time and space the Fermi surface also distorts periodically in time and space. This is often referred to as "breathing Fermi surface." The effort of electrons to repopulate the changing Fermi surface is delayed by a finite relaxation time τ of electrons and this results in a phase lag between the Fermi surface distortions and precessing magnetization. This is a typical scenario for frictional damping. The interband transitions are connected with dynamic orbital polarization, i.e., changes of the electron wave functions beside changes of their energies.

The above equations for the intrinsic damping are not intended for real calculations. They just show the underlying ideas and parameters entering the intrinsic damping in metals. This picture is simple and easier to follow than the existing more detailed theory. Complete calculations using a more sophisticated treatment of spin orbit interaction can be found in [19] and [15]. Recently, Kuneš and Kamberský [20] carried out first principles electronic band calculations of the intraband (breathing Fermi surface) Gilbert damping in Ni, Co, and Fe. They found a good quantitative agreement between the experimental data and their calculations. Experimentally, in Ni the Gilbert damping was found significantly increased when approaching the cryogenic range of temperatures and saturated below 50 K [21]. The saturation of G was explained in [22]. With an increasing $\hbar/\tau$ the energy balance $\hbar\omega - \hbar^2/2m(2\mathbf{kq} + q^2)$ in the denominator of (10) becomes eventually comparable to $\hbar/\tau$. Momentum and energy conservation now play an important role in the sum over the Fermi surface for the intraband Gilbert damping and one finds

$$G \sim \frac{\tan^{-1}\left(qv_F\tau_{orb}\right)}{qv_F} \qquad (13)$$

where q is the wave number of a resonant magnon. For $v_F\tau \gg 1/q$, the expression in (13) saturates and inversely depends on q. This behavior was already well known for the anomalous skin depth where only electrons moving in the skin depth contribute to the conductivity. This effect is usually referred to as the concept of ineffectivness of electrons [23]. The presence of ineffective electrons at low temperatures in the measured Gilbert damping shows very explicitly that the magnetic damping in metallic ferromagnets is caused by itinerant electrons. This is further supported by ferromagnetic antiresonance (FMAR) studies. By using microwave transmission at FMAR ($q \rightarrow 0$), we were able to avoid problems associated with ineffective electrons [24] and get precise values of the intrinsic damping. We found that in high-purity single-crystal slabs of Ni the Gilbert damping below RT was well described by the two terms which were equal in strength and proportional to the conductivity and resistivity [24]. This is in good agreement with the predictions of (11) and (12). Kambersky [25] recently calculated the temperature dependence of the Gilbert damping in Ni. He obtained a reasonable agreement with the FMAR results of [24], [26].

III. Magnetic Relaxations in Multilayers

The role of interface damping was investigated in high quality crystalline Au–Fe–Au–Fe(001) structures grown on GaAs(001) substrates, see details in [27]. The in-plane FMR experiments were carried out using 10, 24 and 36 GHz systems [28]. The in-plane resonance fields and resonance linewidths were measured as a function of the azimuthal angle φ between the external dc magnetic field and the Fe in-plane cubic axis.

Single Fe ultrathin films with thicknesses of 8, 11, 16, 21, and 31 monolayers (MLs) were grown directly on GaAs(001). They were covered by a 20-ML-thick Au(001) cap layer for protection in ambient conditions. FMR measurements were used to determine the in-plane four-fold and uniaxial magnetic anisotropies, K_1 and K_u and the effective demagnetizing field perpendicular to the film surface, $4\pi M_{\rm eff}$, as a function of the film thickness d[28]. The magnetic anisotropies are well described by a linear dependance on $1/d$. The constant and linear terms represent the bulk and interface magnetic properties, respectively. The ultrathin Fe films grown on GaAs(001) have their magnetic properties nearly equal to those in the bulk Fe, modified only by sharply defined interface anisotropies, indicating that the Fe layers are of a high crystalline quality with well defined interfaces. The lineshape of the FMR peaks is Lorentzian and the FMR linewidths are small (under 100 Oe for our microwave frequencies) and only weakly dependent on the film thickness. The reproducible magnetic anisotropies and small FMR linewidths provided an excellent opportunity for investigation of the nonlocal relaxation processes in magnetic multilayer films.

The thin Fe films which were studied in the single-layer structures were regrown as a part of magnetic double layer structures. The thin Fe film (F2) was separated from the second thick Fe layer (F1) of 40-ML thickness by a 40-ML-thick Au normal metal (NM) spacer. The magnetic double layers were covered by a 20-ML Au(001) layer for protection under ambient conditions. The thickness of the Au spacer layer was much smaller than its electron mean free path (38 nm) [29] and hence allowed ballistic electron transfer between the magnetic layers.

The interface magnetic anisotropies separated the FMR fields of F1 and F2 by a big margin, see [27]. That allowed us to carry out FMR measurements in F2 with F1 possessing a negligible angle of precession compared to that in F2. The FMR linewidths in single and double layer structures were only weakly dependent on the azimuthal angle φ of the saturation magnetization with respect to the in-plane crystallographic axes.

The thin Fe film in the single and double layer structures had the same FMR field showing that the interlayer exchange coupling [3] through the 40 ML thick Au spacer was negligible and the magnetic properties of the Fe films grown by MBE on well prepared GaAs(001) substrates were fully reproducible.

The FMR linewidth in F2 always increased in the presence of F2. The additional FMR linewidth, $\Delta H_{\rm add}$, followed an inverse dependence on the thin film thickness d, see Fig. 1(a). This means the nonlocal Gilbert damping originates at the F2/NM interface. The linear dependence of $\Delta H_{\rm add}$ on the microwave frequency for both the parallel and perpendicular configuration with no zero-frequency offset; Fig. 1(b) is equally important. This means that the additional contribution to the FMR linewidth can be described by an interface Gilbert damping. The additional Gilbert damping for the 16-ML-thick film was found to be weakly dependent on the crystallographic direction, $G_{\rm add} = 1.2 \times 10^8\ {\rm s}^{-1}$ along the cubic axis. The strength is comparable to the intrinsic Gilbert damping in the single Fe film, $G = 1.5 \times 10^8\ {\rm s}^{-1}$

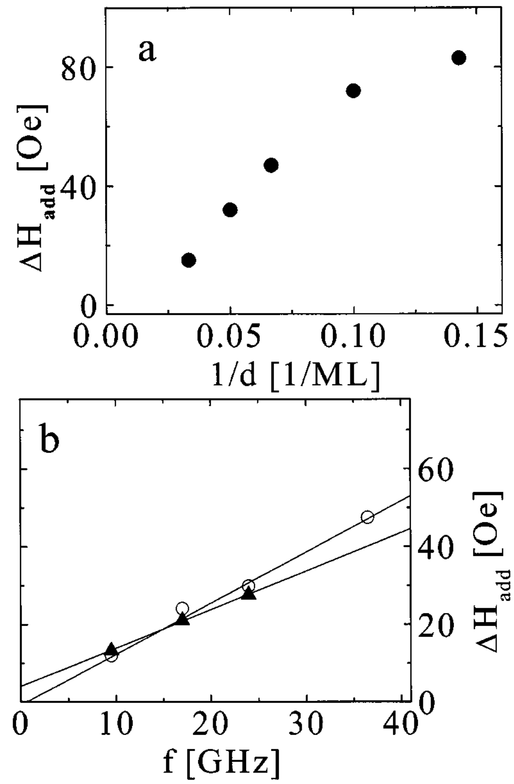

Fig. 1. (a) The dependence of the additional FMR linewidth (in parallel configuration) $\Delta H_{\rm add}$ on $1/d$ at $f = 36$ GHz. d is the thickness of F2. (b) The frequency dependence of $\Delta H_{\rm add}$ for the parallel (open circles) and perpendicular (black triangles) FMR measurements. The measurements were carried out on a GaAs–16Fe–40Au–40Fe–20Au(001) structure grown by MBE. The integers represent the number of ML. The magnetic properties of the Fe layers are shown in [27].

The nonlocal damping observed in the aforementioned multilayer films is in agreement with recent predictions of interface damping by Berger [30], [31]. Berger evaluated the role of the s-d exchange interaction in magnetic double layers assuming that the layer F1 is nearly static and the direction of its magnetic moment determined the axis of the static equilibrium. Magnons were introduced by allowing the magnetic moment in F2 to precess around the equilibrium direction. Itinerant electrons entering the thin ferromagnetic layer through a sharp interface cannot immediately accommodate the direction of the precessing magnetization. Berger showed that this leads to an additional exchange torque which is directed toward the equilibrium axis and represents an additional relaxation term. This relaxation torque is confined to the vicinity of the F2/NM interface. The resulting relaxation torque in a magnetic double layer structure contributes to an additional FMR linewidth [30], $\Delta H_{\rm add}$, which is in the perpendicular configuration proportional to

$$\Delta H_{\rm add} \sim (\Delta\mu + \hbar\omega) \quad (14)$$

where $\Delta\mu = \Delta\mu_\uparrow - \Delta\mu_\downarrow$ is the difference in the majority and minority Fermi level shifts and ω is the microwave angular frequency.

An alternative theory of interface damping was proposed in [32]. In their theoretical treatment, the precessing magnetization at the ferromagnet (FM) /normal metal (NM) interface acts as a "spin pump." The precessing magnetization creates a spin current which propagates away from the FM/NM interface. The spin current in their calculations is valid when the injected spin momentum into a normal metal decays or leaves the interface sufficiently fast to avoid the flow of spin current back into the ferromagnet. In our case, layer F2 acts as a "spin pump." The spin current is given by

$$\mathbf{I}_{sc} = \frac{\hbar}{4\pi} A_r \mathbf{m} \times \frac{\partial \mathbf{m}}{\partial t} \quad (15)$$

where A_r is the scattering matrix and $\mathbf{m} = \mathbf{M}/M_s$ is the unit vector of precessing magnetic moment; see [32]. Note that the spin current has the form of Gilbert damping torque. Now another important question has to be answered: how is the generated spin current disposed? This answer can be found in [33], where it is shown that the transversal component of the spin current in a normal layer is entirely absorbed when it encounters the interface with a ferromagnet. For small precessional angles the spin current $\mathbf{I}_{sc}$ is almost entirely transversal to the magnetic moment of F1, see (15). It means that the NM/F1 interface acts as an ideal spin sink and provides an effective spin brake for F2. The resulting relaxation torque is Gilbert like and that is in perfect agreement with our results.

The study of nonlocal damping provides useful information about the effectiveness of the spin transport in multilayer films which affects the spin dynamics. The experimental verification of the interface Gilbert damping has important implications for spin dynamics in magnetic multilayers. It offers a direct access for experimental measurements of relaxation torques caused by the transfer of electron angular momentum across a nonmagnetic spacer. It also has a practical implication. It would allow one to test the suitability of magnetic unpatterned multilayers for their use in systems employing magnetization precession and switching processes in mesoscopic SWASER devices. Berger used the term "spin wave amplification by stimulated emission of radiation (SWASER)" to describe a device which uses a current induced negative term of damping. $\Delta\mu = \Delta\mu_\uparrow - \Delta\mu_\downarrow$ in (14) can be controlled by an dc applied current passing through the film interfaces [34], [35]. This term involves the spin transfer by conduction processes resulting in a net exchange relaxation torque which is proportional to the current density and can be adjusted to be positive or negative by controlling the direction of applied current. Negative magnetic damping can be obtained by a using large enough current density to overcome the total Gilbert damping of the layer F2. Our results of interface Gilbert damping can be used to determine the critical current which would be required to create a spin dynamics instability (negative damping) in a 16-ML-thick Fe film. At 36 GHz, $\hbar\omega = 0.15$ meV and the nonlocal FMR linewidth was 50 Oe. The total FMR linewidth was 120 Oe. In order to overcome the total Gilbert damping, one needs to get $\Delta\mu = -0.15 \cdot 120/50 = -0.36$ meV. Using the dependence between the current density and $\Delta\mu$ from Berger's ballistic calculations [35] that results in a critical current density of 2.7×10^7 A/cm^2.

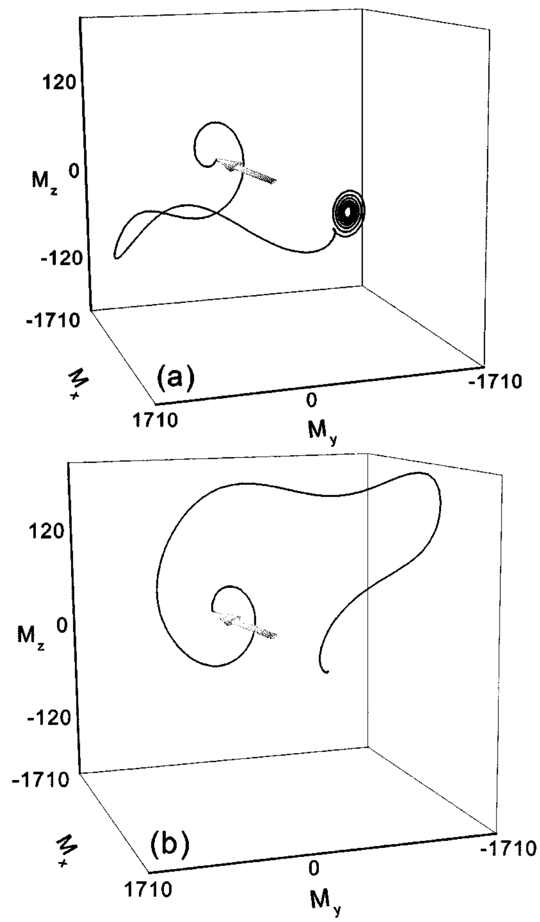

Fig. 2. Time evolution of the magnetic moment in zero external field using Slonczewski's current induced torque, see [34]. Simulations were carried out using the electric current density of 6×10^8 A/cm^{-2} with a pulse duration of 0.5 ns. The magnetic parameters for the dynamic layer F2 are as follow: $4\pi M_s = 21.4$ kG, $4\pi M_{\rm eff} = 18$ kOe, the in-plane four-fold anisotropy $K_1 = 3.5 \times 10^5$ ergs/cm^3, the in-plane uniaxial anisotropy $K_u = -1.0 \times 10^5$ ergs/cm^3, $\alpha = 0.01$ and the g-factor $g = 2.09$. The in-plane uniaxial anisotropy axis is oriented 45° with respect to the cubic crystallographic axis [100]. The stationary layer F1 has its magnetic moment along the [100] crystallographic direction. (a) Includes all magnetic anisotropies. (b) Excludes the in plane uniaxial anisotropy. Note, that the magnetic moment in (a) continued to precess after the current was switched off. This is caused by the in-plane uniaxial anisotropy which rotates the easy axis several degrees away from the [100] crystallographic direction. The current induced torque tilts the magnetic easy axis in F2 closer to the $[\bar{1}00]$ direction and consequently after the current is switched off the magnetic moment in F2 starts to precess toward its own easy axis which is unaffected by the applied current. Note, that the magnetization reversal with the current induced torque is significantly faster than the relaxation purely driven by Gilbert damping. In (b), the uniaxial anisotropy is absent and the final static state is oriented along the easy $[\bar{1}00]$ crystallographic direction. In this case the current driven equilibrium is identical to that given by the magnetic anisotropies and consequently no additional relaxation took place after the current was switched off.

A. Numerical Simulations of Current Driven Spin Instabilities

By applying an external current, one can set two types of instabilities: 1) Magnetization reversal and 2) stationary precessional motion. Using the magnetic properties of the studied Au–Fe–Au–Fe–GaAs(001) magnetic double layers and the interface relaxation torque from [34], computer simulations of

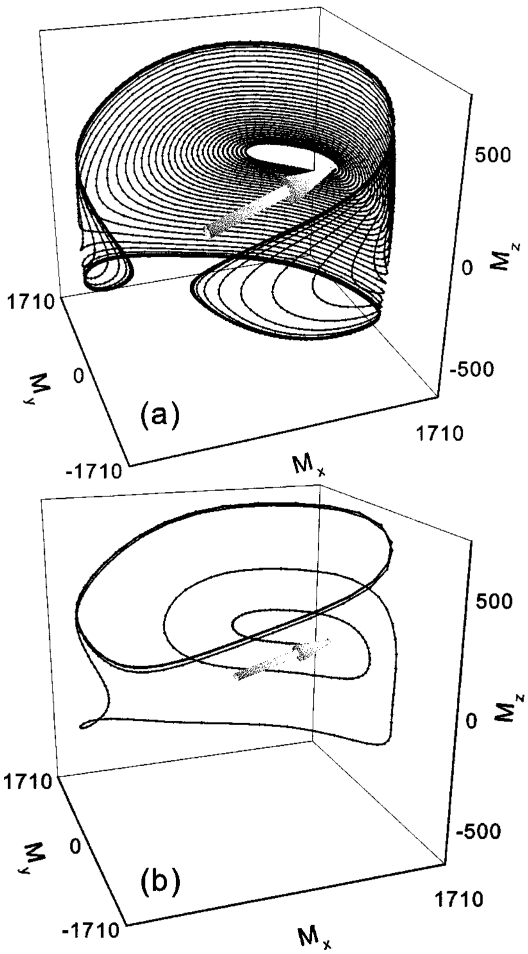

Fig. 3. Time evolution of the magnetic moment in an external field $H = 0.6$ kOe which is applied along the uniaxial easy magnetic axes [110]. The starting orientation of the magnetic moment was a few degrees away from the easy uniaxial axis [110], see the arrow. Computer simulations were carried out with the following current densities: (a) 3.5×10^7 A/cm^{-2} and (b) 2.5×10^8A/cm^{-2}. The magnetic properties of layer F2 are described in Fig. 2. Note, that one is able to establish complex stationary precessions with large amplitudes. For a low current density in (a) the tip of the magnetization follows the edge of a "bracelet." With an increasing current, the bracelet closes and eventually evolves into a "lasso shape" orbit; see (b).

these two processes are shown in Figs. 2 and 3. Note that a large stationary amplitude of the precessing magnetization can be established by using a reasonable current density.

ACKNOWLEDGMENT

B. Heinrich would like to thank the Alexander von Humboldt Foundation and Max Planck Institute in Halle for the support during his research stay in Germany. The authors would also like to thank K. Myrtle for technical assistance, and A. Brataas, E. Simanek, L. Berger, J. F. Cochran, Y. Tserkovnyak, and V. Kamberský for valuable discussions.

REFERENCES

[1] J. R. MacDonald, *Proc. Phys. Soc. A*, vol. 64, pp. 968–983, 1951.
[2] B. Heinrich and J. A. C. Bland, *Magnetic Ultrathin Film Structures II*. New York: Springer-Verlag, 1993.
[3] B. Heinrich and J. F. Cochran, "Ultrathin metallic magnetic films: Magnetic anisotropies and exchange interaction," *Adv. Phys.*, vol. 42, pp. 523–639, 1993.
[4] B. Heinrich, J. F. Cochran, and M. Kowalewski, *Frontiers of Magnetism in Reduced Dimension Systems*, P. Wigen, V. Baryachtiar, and N. Lesnik, Eds. Crimea, Ukraine: NATO-ASI, 1996, ch. V, pp. 161–210.
[5] B. Heinrich and A. S. Arrott, "Evaluation of spin-orbit and dipole-dipole contributions," *J. Appl. Phys.*, vol. 57, pp. 3709–3711, 1985.
[6] B. Heinrich, D. Fraitová, and V. Kamberský, "The influence of s-d exchange on relaxation of magnons in metals," *Phys. Stat. Sol.*, vol. 23, pp. 501–507, 1967.
[7] Z. Frait and D. Fraitova, "Ferromagnetic resonance and surface anisotropy in iron single crystals," *J. Mag. Mag. Mater.*, vol. 15–18, p. 1081, 1980.
[8] ——, *Frontiers of Magnetism in Reduced Dimension Systems*, P. Wigen, V. Baryachtiar, and N. Lesnik, Eds. Crimea, Ukraine: NATO-ASI, 1996, ch. IV, pp. 121–151.
[9] J. F. Cochran, B. Heinrich, and A. S. Arrott, "FMR in systems composed of a ferromagnetic substrate and exchange coupled film," *Phys. Rev. B*, vol. 34, pp. 7788–7801, 1986.
[10] N. Chan, V. Kambersky, and D. Fraitova, "Impedance matrix of thin metallic ferromagnetic films and SSWR in parallel configuration," *J. Mag. Mag. Mater.*, vol. 214, pp. 93–98, 2000.
[11] H. Suhl, "Theory of the magnetic damping constant," *IEEE Trans. Magn.*, vol. 34, p. 1834, 1998.
[12] B. Heinrich, J. F. Cochran, and K. Myrtle, "The exchange splitting of phonon assisted microwave transmission at 9.5 GHz," *J. Appl. Phys.*, vol. 53, pp. 2092–2094, 1982.
[13] T. Kobayashi, R. C. Barker, and A. Yelon, "Ferromagnetic resonance in thin films II: Application to Ni," *Phys. Rev. B*, vol. 7, pp. 3286–3297, 1973.
[14] B. Heinrich, R. Urban, and G. Woltersdorf, "Magnetic relaxations in metallic films. single and double layer structures," *J. Appl. Phys.*, submitted for publication.
[15] V. Kambersky, "On ferromagnetic resonance damping in metals," *Czech. J. Phys.*, vol. B26, pp. 1366–1383, 1976.
[16] D. N. Zubarev, *Sov. Phys. Usp.*, vol. 3, pp. 320–333, 1960.
[17] K. Baberschke, "The magnetism of nickel monolayers," *Appl. Phys. A*, vol. 62, pp. 417–427, 1996.
[18] V. Kamberský, "On the Landau-Lifshitz relaxation in ferromagnetic metals," *Can. J. Phys.*, vol. 48, pp. 2906–2911, 1970.
[19] V. Kambersky, "FMR linewidth and disorder in metals," *Czech. J. Phys.*, vol. 34, pp. 1111–1124, 1984.
[20] J. Kunes and V. Kambersky, First-principles investigation of the damping of fast magnetization precession in ferromagnetic 3d metals, in *Phys. Rev. B*, 2002, submitted for publication.
[21] S. M. Bhagat and P. Lubitz, "Temperature variation of ferromagnetic relaxation in the 3-D transition metals," *Phys. Rev. B*, vol. 10, pp. 179–185, 1974.
[22] V. Korenman and R. E. Prange, "Anomalous damping of spin waves in magnetic metals," *Phys. Rev. B*, vol. 6, pp. 2769–2777, 1972.
[23] J. M. Ziman, *Principles of the Theory of Solids*, 2nd ed. Cambridge, U.K.: Cambridge Univ. Press, 1972, ch. 8.7, p. 607.
[24] B. Heinrich, D. J. Meredith, and J. F. Cochran, "Wave number and temperature dependent Landau-Lifshitz damping in nickel," *J. Appl. Phys.*, vol. 50, pp. 7726–7728, 1979.
[25] V. Kambersky, private communication.
[26] G. Dewar, B. Heinrich, and J. F. Cochran, "Ferromagnetic antiresonance transmission of 24 GHz radiation through nickel (20 to 364 degrees C)," *Can. J. Phys.*, vol. 55, pp. 821–833, 1977.
[27] R. Urban, G. Woltersdorf, and B. Heinrich, "Gilbert damping in single and multilayer ultrathin films: Role of interfaces in nonlocal spin dynamics," Phys. Rev. Lett., vol. 87, 2001, submitted for publication.
[28] B. Heinrich and J. A. C. Bland, *Ultrathin Magnetic Structures II*. New York: Spinger-Verlag, 1994, sec. Radio Frequency Techniques.
[29] A. Enders, T. Monchesky, K. Myrtle, R. Urban, B. Heinrich, J. Kirschner, X.-G. Zhang, and W. H. Butler, "The role of interfaces in the magnetoresistance of Au–Fe–Au–Fe–GaAs(001) ultrathin film structures," *J. Appl. Phys.*, vol. 89, pp. 7110–7112, 2001.
[30] L. Berger, "Emission of spin waves by a magnetic multilayer traversed by a current," *Phys. Rev. B*, vol. 54, pp. 9353–9358, 1996.
[31] ——, "Efect of interfaces on Gilbert damping and FMR linewidth in magnetic multilayers," *J. Appl. Phys.*, vol. 90, pp. 4632–4638, 2001.
[32] Y. Tserkovnyak, A. Brattas, and G. E. W. Bauer, "Enhanced Gilbert damping in thin ferromagnetic films," *Phys. Rev. Lett.*, vol. 88, p. 11 760, 2002.
[33] M. D. Stiles and A. Zangwill, "Anatomy of spin-transfer torque,", submitted for publication.
[34] J. C. Slonczewski, "Current-driven excitation of magnetic multilayers," *J. Magn. Magn. Mater.*, vol. 159, pp. 1–7, 1996.
[35] L. Berger, "New origin for spin current and current induced spin precession in magnitic multilayers," *J. Appl. Phys.*, vol. 89, pp. 5521–5525, 2001.